

Numerical simulation of electrical conductivity in microscopically inhomogeneous materials

Itzhak Webman and Joshua Jortner

Department of Chemistry, Tel-Aviv University, Tel-Aviv, Israel

Morrel H. Cohen

The James Franck Institute and Department of Physics, The University of Chicago, Chicago, Illinois 60637

(Received 23 December 1974)

The electrical transport properties of some microscopically inhomogeneous disordered materials were simulated by numerical calculations of the conductivity of cubic resistor networks with correlated bonds, both above and below the percolation threshold. The major effect of increasingly strong correlation among the metallic bonds is to shift the percolation threshold to lower values of the allowed metallic volume fraction, resulting in $C^* = 0.15 \pm 0.02$ for the continuous-percolation limit. The numerical data were utilized for a quantitative fit of the electrical-conductivity data of metal-ammonia solutions and of alkali-tungsten bronzes, which undergo a continuous metal-nonmetal transition via the inhomogeneous transport regime.

I. INTRODUCTION

The physical picture for continuous metal-nonmetal transitions in some disordered materials¹⁻⁵ rests on the notion that, as a consequence of fluctuations, the material becomes microscopically inhomogeneous with regard to electron transport. Provided that the Debye short correlation length b for fluctuations is long compared to the phase coherence length for the conduction electrons and that tunneling corrections can be disregarded, semiclassical transport theory is applicable. The problem then reduces to that of percolation⁶⁻¹⁵ of classical particles in a random potential. The material is viewed as consisting of a random sub-microscopic mixture of metallic and nonmetallic regions. Let C be the fraction of the total volume which is allowed (or metallic) at the Fermi energy. When C is sufficiently large, continuous metallic paths extend throughout the material, so that electrons at the Fermi energy are in extended states. When C decreases to some critical value C^* , the percolation threshold, extended metallic paths cease to exist, whereupon the condition for localization in the disordered system is $C = C^*$.

Classical percolation theory has to be extended in two directions before it can be applied to the study of transport properties in the inhomogeneous regime. First, one has to consider the continuous-percolation problem in addition to discrete-lattice models. In this context, Scher and Zallen¹⁴ have proposed that for all three-dimensional lattices $C^* = fp_c$, where f is the packing fraction and p_c is the critical site concentration for that lattice. These considerations led to the value of $C^* = 0.15$ in the continuous-percolation problem. Numerical studies by Skal *et al.*¹⁶ of the percolation probability $P(C)$ for a particular random potential in a cubic lattice, with site correlation extending up

the third nearest neighbors, resulted in the asymptotic value of $C^* = 0.17$. Second, a proper semiclassical theory of the transport properties has to be developed. It was demonstrated by three elegant table-top experiments,¹⁸⁻²⁰ that transport properties, such as the electrical conductivity $\sigma(C)$, cannot be directly related to $P(C)$. Kirkpatrick¹⁷ has carried out extensive numerical studies of the conductivity of a simple-cubic resistor network, in which each nearest-neighbor bond was randomly assigned a conductance $\sigma(1)$ with the probability C and $\sigma(0)$ with the probability $1 - C$. He found that the effective-medium theory (EMT)²¹⁻²⁶ was accurate for $0.4 < C < 1$ for all values of the conductivity ratio $x = \sigma(0)/\sigma(1)$. However, serious deviations from the EMT occurred for $C < 0.4$ for small values of x (< 0.01). In the limit of $x = 0$, the current flow within the resistor network reduces to a bond percolation problem, for which the percolation threshold is $C^* = 0.25$ and where numerical calculation results in¹⁷

$$\sigma(C) = 0, \quad C < C^* \quad (1.1a)$$

$$\sigma(C) = A(C - C^*)^\gamma, \quad C^* < C < 0.4, \quad \gamma = 1.6 \quad (1.1b)$$

$$\sigma(C) = \sigma(1)(\frac{3}{2}C - \frac{1}{2}), \quad 0.4 < C; \quad (1.1c)$$

EMT gives

$$\sigma(C) = 0, \quad C < \frac{1}{3}$$

$$\sigma(C) = \sigma(1)(\frac{3}{2}C - \frac{1}{2}); \quad C > \frac{1}{3}. \quad (1.2)$$

Thus the EMT overestimates the value of the percolation threshold for $x = 0$, and can, in general, be expected to result in too low values of $\sigma(C)$ for $C < 0.4$ and $x \neq 0$.

The failure of the EMT near the percolation threshold precludes its quantitative application to the problem of electron transport in the vicinity of the metal-nonmetal transition. It is apparent that

either an improved formal theory has to be developed for $C < 0.4$ and $x < 0.01$ or that one has to rely on the results of numerical simulations. Yonezawa and Hori^{27,28} have recently advanced a formal treatment for a sc lattice which improves the EMT. The extension of this procedure to other lattices is straightforward. It is, however, not clear whether this theory is applicable for the continuous-percolation problem. Concerning numerical simulations, one can utilize Kirkpatrick's scaling law,¹⁷ Eq. (1.1b), with the value $C^* = 0.17$ to estimate σ above the percolation threshold for low values of x ($< 10^{-4}$). A quantitative fit of the transport data of inhomogeneous materials requires, however, detailed information concerning $\sigma(C)$ both above and below C^* . In simulating the electrical transport properties of a microscopically inhomogeneous material, we are dealing with a continuous-site-percolation problem, in which any portion of the material can be randomly metallic or nonmetallic. Such a continuous-percolation problem has to be regarded as the limit of either site or bond percolation on any lattice as the maximum allowed bond length increases relative to nearest-neighbor separation. Alternatively, one can impose correlations on neighboring bonds, so that if a bond is of one type all its neighbors out to a given correlation distance must be of the same type. This correlation distance should be taken to be equal to b . As the latter procedure closely resembles what occurs in disordered materials, we have undertaken a numerical study of the conductivity of a simple-cubic resistor network with correlated bonds. The major effect of these correlations is to shift the percolation threshold from $C^* = 0.25$ to 0.15 ± 0.02 , in accord with the previous numerical simulations of $P(C)$ for continuous percolation.^{14,16} For low x ($< 10^{-4}$) values the scaling law (1.1b) with $\gamma = 1.6 \pm 0.2$ is retained, while for $C > 0.5$ for all x , the data are found to faithfully reproduce the EMT results. These features confirm Kirkpatrick's conclusions¹⁷ under more general circumstances. A study of the conductivity data in the range $0 < C < C^*$ results in the relation $\sigma = \sigma(0)/(1 - \alpha C)$, where $\alpha = 1/C^*$ (within an uncertainty range of 0.02). This last result is of interest for the elucidation of the transport properties in the pseudosemiconducting regime. Our numerical results yield detailed information concerning $\sigma(C)$ for small values of C ($0 < C < 0.5$) and of x ($0 < x < 0.05$) which will be useful for the quantitative analysis of transport properties in inhomogeneous materials. We shall discuss briefly the applications of our numerical results for the analysis of the conductivity of two systems, metal-ammonia solutions and alkali-tungsten bronzes, which exhibit continuous metal-nonmetal transition via the inhomogeneous-transport regime.

II. CORRELATED RESISTOR NETWORK MODELS

Provided that the Debye short correlation length for fluctuations exceeds both the internuclear spacing and the phase coherence length of the conduction electrons, a local conductivity $\sigma(\vec{r})$ can be defined,¹⁻⁵ relating the microscopic current density $\vec{j}(\vec{r})$ to the microscopic electric field $\vec{E}(\vec{r})$:

$$\vec{j}(\vec{r}) = \sigma(\vec{r})\vec{E}(\vec{r}). \quad (2.1)$$

This equation may be solved using a finite difference approximation. Introducing a regular cubic mesh of points $\{\vec{r}_i\}$ with spacing $\delta\vec{r}$, one obtains a system of linear equations

$$\sum_j g_{ij}(V_i - V_j) = 0, \quad (2.2)$$

where

$$g_{ij} = \delta r \sigma(\frac{1}{2}(\vec{r}_i + \vec{r}_j)). \quad (2.3)$$

V_i is the potential at $r = r_i$. Equation (2.2) holds for all r_i not at the surface and i and j correspond to neighboring sites in the mesh. Kirkpatrick^{11,12,17} has pointed out that Eq. (2.2) is equivalent to the Kirchoff current law for a regular network of random values conductances g_{ij} . Following Kirkpatrick,^{11,12,17} we have considered a three-dimensional sc array of resistors. The electrodes are parallel to two faces of the cube. For the other faces cyclic boundary conditions are imposed by connecting pairs of points on the opposite faces through random conductances. In the original work^{11,12,17} the fractions C and $1 - C$ of the bonds are randomly assigned the values $g_{ij} = 1$ and $g_{ij} = x$, respectively. This was accomplished by assigning to each bond a random number $0 < r < 1$. Then all bonds for which r falls within a preselected interval are given the value $g_{ij} = x$ while the others are characterized by $g_{ij} = 1$. We have used a modification of Kirkpatrick's original program, which improved convergence and incorporated bond correlation.

The set of N^3 equations (2.2) was solved by the Gauss-Seidel relaxation procedure

$$V_i^{(n)} = \frac{\sum_{j < i} g_{ij} V_j^{(n)} + \sum_{j > i} g_{ij} V_j^{(n-1)}}{\sum_j g_{ij}}, \quad (2.4)$$

where n specifies the number of the iteration and $j < i$ implies that the equation for V_j precedes the one for V_i in the loop over the sites. After the relaxation procedure converges, the current in the direction of the average field is evaluated. Assigning the value of unity to the potential differences between the electrodes, the current is equal to the numerical value of $\sigma(C)$. The solution converges rapidly for C above the transition region, but many iterations are required around and below C^* . When correlations between the locations of high

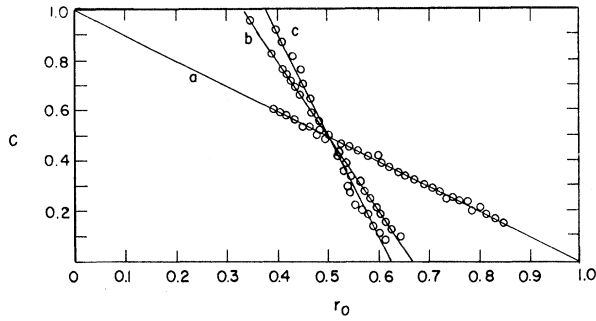


FIG. 1. Concentration of metallic bonds plotted against the prescribed number r_0 : (a) noncorrelated network; (b) nearest-bond correlated network; (c) second-order correlated network.

and low conductivity bonds are incorporated, an over-relaxation procedure improved the convergence by an order of magnitude. The over-relaxed²⁵ equations can be recast in the form

$$V_i^{(n)} = (1 - \Omega)V_i^{(n-1)} + \Omega \frac{\sum_{j < i} g_{ij} V_j^{(n)} + \sum_{j > i} g_{ij} V_j^{(n-1)}}{\sum_{j} g_{ij}} \quad (2.5)$$

values of Ω between 1.6 and 1.9 proved to be effective.

To explore the consequences of bond correlation effects on $\sigma(C)$ we have considered three different models which involve increasingly strong correlations among the bonds.

Model A: Nearest-neighbor bond correlation. This was constructed by assigning a random number r to each bond. Then the six bond numbers associated with each vertex were averaged resulting in a new set of numbers r' . All bonds leading to a vertex were assigned the value r' for that vertex, unless values of r' were previously assigned from vertices considered earlier. The value of $g_{ij} = 1$ was then assigned to the conduc-

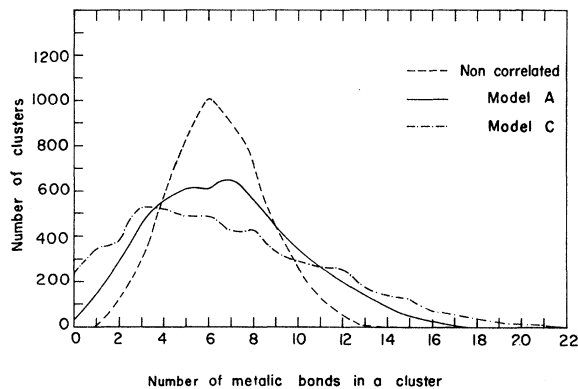


FIG. 2. Distribution of vertex points with $0 < n < 22$ metallic bonds in a cluster of 22 bonds surrounding the vertex.

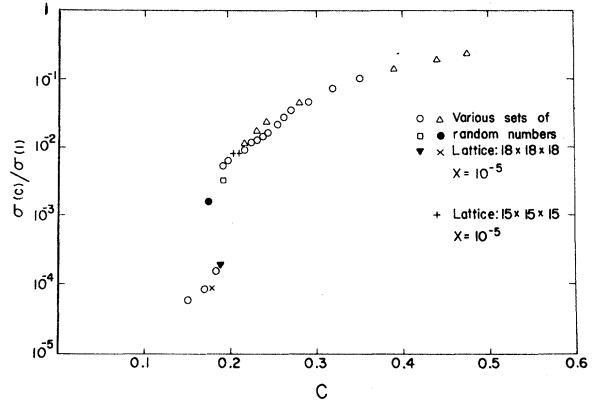


FIG. 3. Numerical results for σ in the transition region for model B obtained using different sets for random numbers.

tance of all the bonds for which $r' > r_0$, where $0 < r_0 < 1$ was a preassigned number. For those bonds where $r' < r_0$, we took $g_{ij} = x$. For the uncorrelated random distribution $\{r\}$, the probability $P(r)$ is constant in the range $0 < r < 1$ and thus $C = 1 - r_0$, as is evident for the numerical data in Fig. 1. The correlated distribution $\{r'\}$ results in a symmetrical distribution function $P(r')$ which peaks about $r' = 0.5$. In this case, as demonstrated by the numerical data in Fig. 1, $C \neq 1 - r_0$. The concentration of metallic bonds is identified with the metallic volume fraction C .

Model B: High conductance clusters. Random numbers $\{r\}$ are assigned to each vertex. If a site is characterized by a value of $r > r_0$ with r_0 being a preassigned value, all the previously unassigned bonds leading to it were all given the value $g_{ij} = 1$, whereas $g_{ij} = x$ was given when $r < r_0$. The concentration of metallic bonds was again determined as in model A.

Model C: Second-order bond correlation. The averaging procedure in model A was iterated once more on the first-order correlated set $\{r'\}$ re-

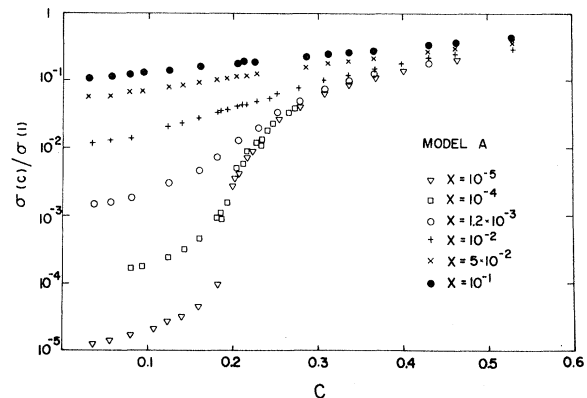


FIG. 4. Numerical results for σ for model A.

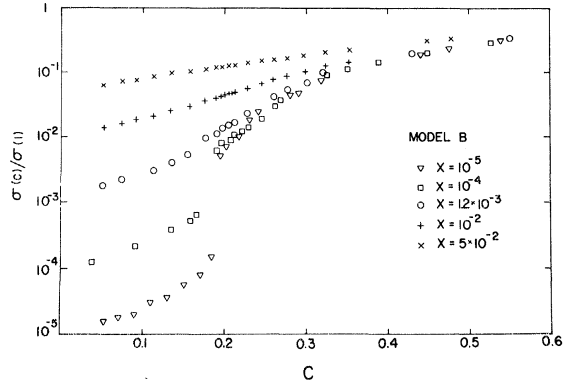


FIG. 5. Numerical results for σ for model B.

sulting in a new set of correlated random numbers $\{r''\}$. We then assigned the values $g_{ij}=1$ for $r'' > r_0$, or $g_{ij}=x$ for $r'' < r_0$, with $0 < r_0 < 1$. The distribution function $P(r'')$ peaks again at about $r'' = 0.5$, and, as is apparent from Fig. 1, $C \neq 1 - r_0$. The counting procedure for the concentration (i.e., the volume fraction C) of metallic bonds was performed as for model A. This second averaging process results in a spatial propagation of the bond correlation.

To demonstrate the effects of the various bond correlation schemes on the distribution of metallic bonds, we have defined a certain configuration of z bonds around each vertex in the lattice and counted the number $N(n)$ of sites for which n out of the z bonds are metallic. Thus $\sum_{n=0}^z N(n)$ is equal to the total number of sites in the lattice. For the uncorrelated system $N(n) = \binom{z}{n} C^n (1-C)^{z-n}$. The histograms portrayed in Fig. 2 for $z=22$ clearly illustrate the increase of the contribution of higher- n values, which is due to the effect of increasingly strong correlation among the bonds.

The numerical studies reported below were performed for an $18 \times 18 \times 18$ network. We have studied the effect of the finite sample size on the stat-

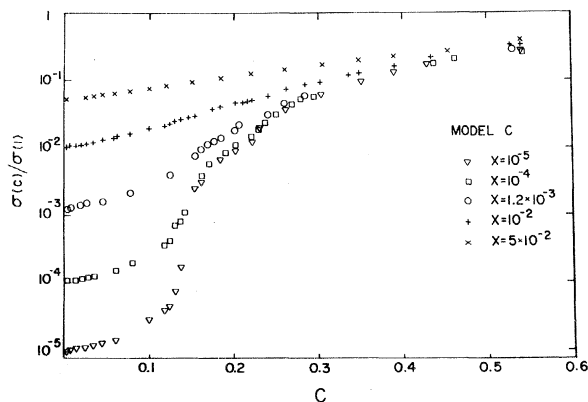


FIG. 6. Numerical results for σ for model C.

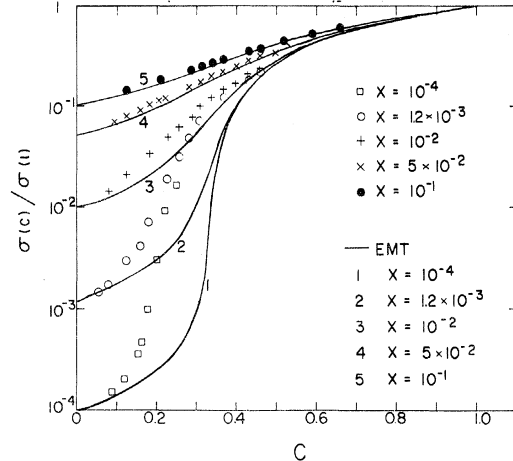


FIG. 7. Comparison of $\sigma(C)^{EMT}$ with the numerical values of obtained for model A.

istical fluctuations in the conductivity data by using different sets of random numbers. The effects of statistical fluctuations (see Fig. 3) are more pronounced near the percolation threshold for low- x ($< 10^{-4}$) values. As expected, the statistical fluctuations in the transition range were somewhat larger for the doubly correlated samples (model C) than for models A and B. We also note that changing the sample size from $15 \times 15 \times 15$ to $18 \times 18 \times 18$ has practically no effect on the numerical results.

III. NUMERICAL STUDIES

Conductivity data for the three bond correlated models are presented in Figs. 4–6. Several features of these results will be now considered.

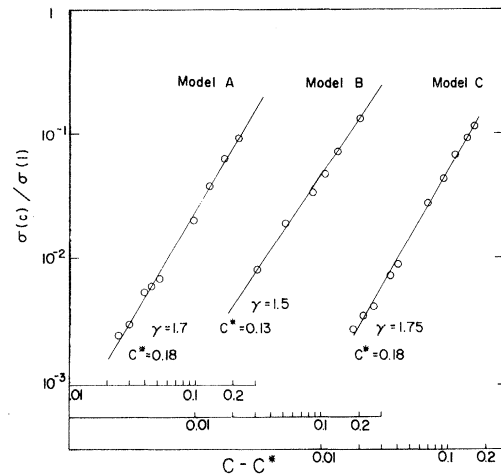


FIG. 8. Log-log plots of σ vs $(C - C^*)$ used for the determination of A and γ in the power law $\sigma(C) = A(C - C^*)^\gamma$ near threshold. The values of A and of γ are summarized in Table I.

TABLE I. Fit of the numerical conductivity data for cubic networks in the region $C^* < C < 0.4$ to the power law $\sigma(C)/\sigma(1) = A(C - C^*)^\gamma$.

Network	Two-parameter fit		Fit with $\gamma = 1.6$		
	γ	C^*	A	C^*	A
Noncorrelated	1.6	0.25	2.9	0.25	2.9
Nearest-bonds correlation (model A)	1.7	0.18	2.3	0.184	2.0
Clusters (model B)	1.5	0.18	1.3	0.183	1.6
Second-order bond correlation (model C)	1.75	0.13	1.2	0.145	1.2

As is evident from Fig. 7, the EMT is accurate for all values of x for high C (> 0.5) and over the whole C range for high x (> 0.05). We thus confirm Kirkpatrick's conclusions concerning the range of validity of the EMT, but now under more general circumstances.

In the transition region $0.1 < C < 0.4$ the results for $x < 0.05$ exhibit a systematic trend towards higher conductivity with increasing degree of correlation. This can be most readily understood by referring to the limit $x \rightarrow 0$, the strict percolation problem. Approaching continuous percolation, by increasing the degree of bond correlation, the percolation threshold decreases from $C^* = 0.25$ for the uncorrelated case to a lower value. We have

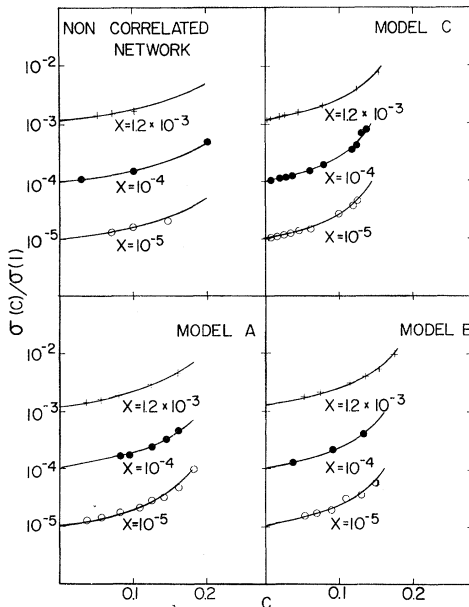


FIG. 9. Fit of numerical values of σ at low C (< 0.15) to the relation $\sigma(C) = \sigma(0)/(1 - \alpha C)$. The best values of α^{-1} are summarized in Table II.

TABLE II. Analysis of conductivity data for low- C ($< C^*$) values for correlated cubic networks. Values of α^{-1} , presented herein, were obtained from the best fits to the numerical results (see Fig. 9) according to Eq. (3.1).

Network	$x = 10^{-5}$	$x = 10^{-4}$	$x = 1.2 \cdot 10^{-3}$
Noncorrelated	0.25	0.25	0.25
Nearest bond correlation (model A)	0.20	0.21	0.22
Clusters (model B)	0.18	0.18	0.20
Second order correlation (model C)	0.16	0.16	0.18

adopted two methods to determine the percolation threshold from the numerical conductivity data at low x ($= 10^{-5}$). First, a fit to Kirkpatrick's scaling law¹⁷ $\sigma(C) = A(C - C^*)^\gamma$ was performed taking for the "best" value for the exponent $\gamma = 1.6$. Second, a two-parameter fit was performed. Figure 8 displays a log-log plot of the conductivity vs $C - C^*$ for several choices of C^* . The best estimate of C^* is taken for that value where the power-law dependence holds over the range $C = 0.2 - 0.4$. From the data summarized in Table I, we conclude that the percolation threshold for the conductivity in bond correlated networks is $C^* = 0.17 \pm 0.01$ for models A and B, slightly decreasing to $C^* = 0.145 \pm 0.02$ with extending the correlation range in model C. The uncertainties in these estimates originates from statistical fluctuations of the data in the transition range. Our data result in the value $C^* = 0.15 \pm 0.02$ for the continuous-percolation limit. This value of C^* , obtained from the conductivity data, practically coincides with the estimate¹⁴ $C^* = 0.15$ and with the numerical result¹⁶ $C^* = 0.17$ obtained for the percolation threshold in the limit of continuous percolation. Our data appear sufficiently reliable to rule out any discrepancy larger than 0.02 between C^* values for $\sigma(C)$ and for $P(C)$. Thus, in analogy to the case of site percolation,¹¹ the continuous-bond-percolation problem should be characterized by a relation of the form $\sigma(C) = P(C)F(C)$, where $F(C) = 0$ for $C < C^*$.

For low- C (< 0.1) values, the EMT results in the asymptotic formula

$$\sigma(C) = \sigma(0)/(1 - \alpha C), \quad (3.1)$$

where $\alpha = 3$. Thus $\alpha = 1/C^*$ since $C^* = \frac{1}{3}$ in the EMT. If we reinterpret Eq. (3.1) by replacing the EMT value of $\alpha = 3$ by the actual value $\alpha = (C^*)^{-1}$ for the correlated networks, a good fit of the numerical data is obtained in the low- C range. The best fits obtained using Eq. (3.1), displayed in Fig. 9 and in Table II, demonstrate that in all cases $\alpha^{-1} = C^*$ within the uncertainty range 0.02 for C^* estimated from the conductivity threshold.

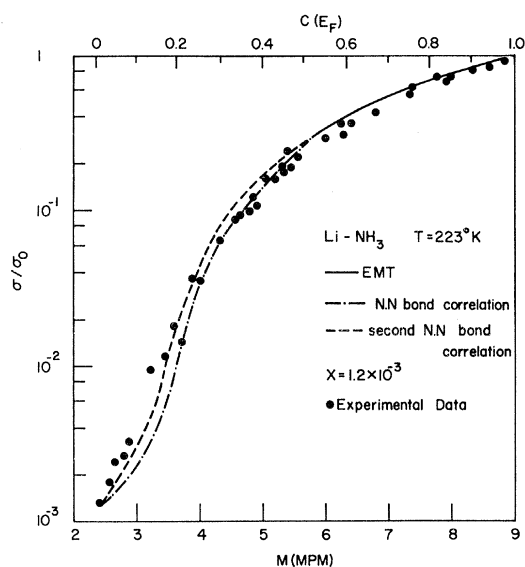


FIG. 10. Analysis of the electrical conductivity of Li-NH₃ solutions at 223 °K. The C scale was obtained from paramagnetic susceptibility data and $x = 1.2 \times 10^{-3}$ (Refs. 3 and 4). Solid line, EMT for $C > 0.5$; dotted-dashed line, model A; dashed line, models B and C which yield practically identical results for this x value. Points represent experimental data (Ref. 36).

IV. ANALYSIS OF CONDUCTIVITY DATA IN SOME MICROSCOPICALLY INHOMOGENEOUS MATERIALS

We now apply the conductivity data obtained herein from numerical simulations to (i) metal-ammonia solutions²⁹ and (ii) alkali-tungsten bronzes³⁰ which undergo a continuous metal-nonmetal transition via the inhomogeneous transport regime. Cohen and Jortner^{3,4} have recently proposed that in Li-NH₃ solutions the metallic propagation regime is separated from a nonmetallic regime by a microscopically inhomogeneous regime where the metal concentration fluctuates locally about either of two well-defined values M_0 and M_1 where $M_0 > M_1$, the local concentration remaining near M_0 or M_1 over radii which are approximately equal to the Debye short correlation length for concentration fluctuations. This physical picture is strongly supported by concentration-fluctuation determinations based on chemical-potential measurements in Li and Na solutions^{31,32} and by small-angle x-ray and neutron-scattering^{33,34} data in Li solutions. The limits of the inhomogeneous regime were determined by a combination of concentration-fluctuation measurements, electrical-conductivity, Hall-effect, and paramagnetic susceptibility data^{35,36} resulting in $M_0 = 9$ mole percent metal (MPM) and $M_1 = 2.3$ MPM for both Li-NH₃ at 223 °K and Na-NH₃ at 240 °K, from the experimental data³⁶ $x = 1.2 \times 10^{-3}$ for Li-NH₃ at 223 °K, resulting in the C

scale, $C = (3M - 7)/20$. We have compared in Fig. 10 the experimental conductivity data of Li-NH₃ solutions with the results of the various numerical simulations. We note that when the correlation length is increased, so that the continuum-percolation limit is approached, the fit is satisfactory over three orders of magnitude of variation in σ . The fit of the experimental data for $C > 0.5$ to the traditional EMT is reasonable, but exhibits a systematic overestimate of $\sigma(C)/\sigma(1)$ which amounts to 20% at $C = 0.5$. The discrepancy is due to boundary scattering effects.^{3,4} On the basis of this analysis, there should be little doubt now as to the existence of the inhomogeneous transport regime in this system.

Alkali-tungsten bronzes, $M_x\text{WO}_3$, are nonstoichiometric compounds, where the alkali metal M at atomic concentration $0 < X < 1$ occupies a simple-cubic sublattice.³⁰ The electrical conductivity, the Hall effect, and the optical data^{30,37-40} indicate the occurrence of an onset of pseudometallic properties for $X = 0.17 \pm 0.02$. A site-percolation model for this system has been advanced by Mackintosh⁴⁰ and by Fuchs.⁴¹ Fuchs has concluded on the basis of paramagnetic susceptibility data that $C = X$. The site-percolation threshold for a sc lattice is $C^* = 0.33$, which is incompatible with the σ data. Lightsey³⁸ has demonstrated the applicability of Kirkpatrick's power law, Eq. (3.1), with $C^* = 0.17$, suggesting that incorporating second- and third-nearest neighbors characterizes a site-percolation problem with an effective coordination number of $z_{\text{eff}} = 14$. It is our view that the metal-nonmetal transition in this system proceeds via an inhomogeneous transport regime, so that electronic transport can be specified in terms of a continuum-percolation process.⁴² This proposal which involves a nonrandom distribution of the interstitial alkali atoms on the sc sublattice, is

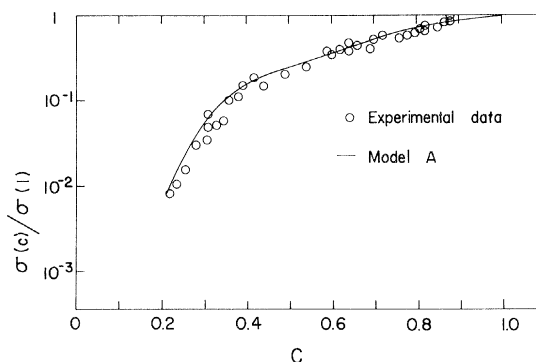


FIG. 11. Analysis of conductivity data of alkali-tungsten bronzes at 300 °K. Experimental data (Refs. 37 and 38) are normalized to $\sigma(1) = 7 \times 10^4$ ($\Omega \text{ cm}$)⁻¹. The solid curve represents results of numerical simulation for model A with $X = 10^{-3}$ for $C > 0.2$.

supported by independent experimental evidence from magnetic data^{43,44} that the metal atoms tend to form preferably into metallic regions. The C scale was established from paramagnetic susceptibility data, taking $C=X$. We note in passing that identifying C with X implies that all the alkali atoms are tied up in metallic clusters. In Fig. 11 the experimental data at 300 °K are compared with the numerical curve of $\sigma(C)$ for a bond correlated lattice. As conductivity data are not available for $C < 0.2$, we have relied on a single point³⁰ at $X=C=0.098$ which indicates that $\sigma(0)/\sigma(1) \leq 10^{-3}$. We have accordingly chosen $\sigma(0)/\sigma(1) = 10^{-3}$. The overall fit is satisfactory, providing a vast improvement over previous transport theories for this system. The systematic overestimate of σ exhibited in this system originates again from scattering effects from the boundaries of the metallic regions. At lower values of C , our results make contact with Lightsey's use³⁸ of Kirkpatrick's power law with $C^* = 0.17$, and our picture of sufficient alkali-metal correlation, $b > a$ (the cube edge), for continuum percolation to hold provides a natural explanation of Lightsey's observation.

It should be recognized that once the limits of the inhomogeneous regime are established from magnetic, thermodynamic, or any other independent data the theoretical curves are fixed to the experimental conductivity data at the $C=0$ and $C=1$ end points of the inhomogeneous range and that otherwise there are no adjustable parameters in the theory (we have ignored boundary scattering corrections^{3,4} in this context). The numerical simulations of reported herein should be regarded as a useful tool for establishing the validity of the inhomogeneous transport picture in some disordered materials.

ACKNOWLEDGMENTS

We are greatly indebted to Scott Kirkpatrick for providing us with his computer program. This research was supported in part by the U.S.-Israel Binational Science Foundation at the University of Tel-Aviv and by the U.S. Army Research Office, ARO(D). We have also benefited from the general support of research provided at The University of Chicago by the Materials Research Laboratory of the National Science Foundation.

-
- ¹M. H. Cohen and J. Jortner, Phys. Rev. Lett. **30**, 699 (1973).
²M. H. Cohen and J. Jortner, Phys. Rev. A **10**, 978 (1974).
³J. Jortner and M. H. Cohen, J. Chem. Phys. **58**, 5170 (1973).
⁴J. Jortner and M. H. Cohen (unpublished).
⁵(a) M. H. Cohen and J. Jortner, in *Proceedings of the Fifth International Conference on Amorphous and Liquid Semiconductors*, Garmisch, Germany, 1973 (Taylor and Francis, London, 1974), p. 167; (b) M. H. Cohen and J. Jortner, J. Phys. (Paris) **35**, C4-345 (1974).
⁶J. M. Ziman, J. Phys. C **1**, 1532 (1968).
⁷S. R. Broadbent and J. M. Hammersley, Proc. Camb. Philos. Soc. **53**, 629 (1957).
⁸H. L. Frisch and J. M. Hammersley, J. Soc. Ind. Appl. Math. **11**, 894 (1963).
⁹J. W. Essam, in *Phase Transition and Critical Phenomena*, edited by C. Domb and M. S. Green (Academic, New York, 1973).
¹⁰V. K. S. Shante and S. Kirkpatrick, Adv. Phys. **20**, 325 (1971).
¹¹S. Kirkpatrick, Rev. Mod. Phys. **45**, 574 (1973).
¹²S. Kirkpatrick, in *Proceedings of the Second International Conference on Liquid Metals*, Tokyo, Japan (Taylor and Francis, London, 1972).
¹³S. Kirkpatrick, Solid State Commun. **12**, 1279 (1973).
¹⁴H. Scher and R. Zallen, J. Chem. Phys. **53**, 3759 (1970).
¹⁵R. Zallen and H. Scher, Phys. Rev. B **4**, 4771 (1971).
¹⁶A. S. Skal, B. I. Shklovski, and A. L. Efros, Zh. Eksp. Teor. Fiz. Pis'ma Red. **17**, 522 (1973) [JETP Lett. **17**, 377 (1973)].
¹⁷S. Kirkpatrick, Phys. Rev. Lett. **27**, 1722 (1971).
¹⁸B. J. Last and D. J. Thouless, Phys. Rev. Lett. **27**, 1719 (1971).
¹⁹D. Adler, L. P. Flora, and S. D. Senturia, Solid State Commun. **12**, 9 (1973).
²⁰J. P. Fitzpatrick, R. B. Malt, and F. Spaepen, Phys. Lett. A **47**, 207 (1974).
²¹D. A. G. Bruggeman, Ann. Phys. (Leipz.) **24**, 636 (1935).
²²R. J. Landauer, J. Appl. Phys. **23**, 779 (1952).
²³V. I. Odehlevskii, J. Tech. Phys. (USSR) **21**, 678 (1951).
²⁴E. H. Kerner, Proc. Phys. Soc. Lond. B **69**, 802 (1956).
²⁵H. J. Juretschke, R. Landauer, and J. A. Swanson, J. Appl. Phys. **27**, 838 (1956).
²⁶M. H. Cohen and J. Jortner, Phys. Rev. Lett. **30**, 696 (1973).
²⁷F. Yonezawa and M. Hori (unpublished).
²⁸M. Hori and F. Yonezawa, J. Math. Phys. (to be published).
²⁹(a) M. H. Cohen and J. C. Thompson, Adv. Phys. **17**, 857 (1968); (b) G. Lepoutre and J. P. Lelieur, in *Metals-Ammonia Solutions*, edited by J. J. Lagowski and M. J. Sienko (Butterworth, London, 1970), p. 369; (c) G. Lepoutre, in *Electrons in Fluids*, edited by J. Jortner and N. R. Kestner (Springer-Verlag, Heidelberg, 1973), p. 193.
³⁰(a) M. J. Sienko, Adv. Chem. Phys. **39**, 224 (1963); (b) H. R. Shanks, P. H. Sidles, and G. C. Danielson, *ibid.* **39**, 237 (1963).
³¹K. Ichikawa and J. C. Thompson, J. Chem. Phys. **59**, 1680 (1973).
³²J. P. Lelieur and J. C. Thompson, J. Phys. (to be published).
³³P. W. Schmidt, J. Chem. Phys. **27**, 23 (1957).
³⁴P. Chieux, Phys. Letters A (to be published).
³⁵J. P. Lelieur, P. Damay, and G. Lepoutre, in Ref. 29(c), p. 203.
³⁶(a) J. A. Schroeder and J. C. Thompson, Phys. Rev.

- 179, 124 (1971); (b) D. S. Kyser and J. C. Thompson, *J. Chem. Phys.* 42, 3910 (1965); (c) R. D. Nasby and J. C. Thompson, *ibid.* 53, 109 (1970); (d) J. A. Vanderhoff and J. C. Thompson, *ibid.* 55, 105 (1971); (e) R. D. Nasby and J. C. Thompson, *ibid.* 49, 696 (1968); (f) J. A. Morgan, J. A. Schroeder, and J. C. Thompson, *ibid.* 43, 4494 (1965); (g) J. A. Schroeder, J. C. Thompson, and P. L. Oertel, *Phys. Rev.* 178, 298 (1969).
- ³⁷(a) B. W. Brown and E. Banks, *Phys. Rev.* 84, 609 (1951); (b) W. R. Gardner and G. C. Danielson, *Phys. Rev.* 93, 46 (1954); (c) C. D. Ellerbeck, H. R. Shanks, P. H. Sidles, and G. C. Danielson, *J. Chem. Phys.* 25, 298 (1961); (d) L. D. Muhlstein and G. C. Danielson, *Phys. Rev.* 158, 825 (1967).
- ³⁸P. A. Lightsey, *Phys. Rev. B* 8, 3586 (1973).
- ³⁹B. A. Brown and E. Banks, *J. Am. Chem. Soc.* 76, 963 (1954).
- ⁴⁰A. R. Mackintosh, *J. Chem. Phys.* 38, 1991 (1963).
- ⁴¹R. Fuchs, *J. Chem. Phys.* 42, 3781 (1965).
- ⁴²J. Jortner, M. H. Cohen and I. Webman (unpublished).
- ⁴³A. T. Fromhold, Jr. and A. Narath, *Phys. Rev.* 136, A487 (1964).
- ⁴⁴A. T. Fromhold, Jr. and A. Narath, *Phys. Rev.* 152, 585 (1966).